Influence of subsurface microstructure on the running-in of an AlSi alloy

D. Linsler [a,b,*], T. Schlarb [a], T. Weingärtner [b], M. Scherge [a,b]

[a] Fraunhofer Institute for Mechanics of Materials IWM, MicroTribology Center μTC, Wöhlerstr. 11, 79108 Freiburg, Germany
[b] Karlsruhe Institute of Technology KIT, Institute for Applied Materials IAM, Hermann-von-Helmholtz-Platz 1, 76344 Eggenstein-Leopoldshafen, Germany

ARTICLE INFO

Keywords:
Lubricated sliding wear
Non-ferrous metals
Electron microscopy
Surface analysis
Tribochemistry

ABSTRACT

The friction and wear behavior of a lubricated AlSi11Cu3 disk in contact with a 100Cr6 pin was studied by a radionuclide assisted pin on disk tribometer. It is well known that shear forces change chemistry and microstructure of the near surface material, thereby influencing friction and wear. To better understand the influences of the microstructure on the running in behavior, disks with different silicon phase morphologies were tested under constant stressing conditions. Topography, chemistry and microstructure of pin and disk were characterized before and after tribological testing by white light interferometry, X ray photoelectron spectroscopy, Auger electron spectroscopy and focused ion beam microscopy. Wear of pins was measured with a radionuclide technique to resolve ultra low wear rates. To characterize near surface deformations, Ga ion markers were implanted and Auger electron spectroscopy was applied to follow their shear induced displacements. To monitor subsurface shear, the deformation of columnar markers was analyzed. The results were discussed using Godet's third body model. Furthermore, the results allowed to us extend the model to systems operated under ultra low wear rates.

1. Introduction

Aluminum silicon alloys have the advantage of being light weight with a high specific strength making them interesting for applications such as pumps or engine blocks. Nevertheless upon sliding, AlSi alloys are subject to plastic deformation at the tribolo gical interface [1,2]. In addition, mechanical intermixing leads to drastic changes of chemical composition and microstructure of the near surface material [3], thereby influencing the running in char acteristics of the system. This is a highly dynamic feed back process which responds very sensitive to external stressing conditions such as load, speed, or temperature [4], but also to the state of the subsurface material [5], mainly pre set by machining and heat treatment of the metals. We differentiate between *near surface* and *subsurface. Near surface* refers to a zone underneath the surface with a thickness up to 1 μm, whereas *subsurface* is used to describe deeper areas of the material. To address these issues and to reduce complex ity, in the present study lubricated disks of AlSi11Cu3 were tested against 100Cr6 pins with a pin on disk tribometer. To illustrate the influence of the initial subsurface microstructure on the running in behavior, disks with and without heat treatment were tested while keeping all other parameters like machining, roughness and test procedure constant. The heat treatment resulted in a different morphology of the silicon grains inside the aluminum matrix.

With respect to modeling, the first comprehensive description of the tribological interface that is received after running in was presented by Godet in the 1980s. This is the so called third body concept [6] linking friction and wear studies to those on lubrica tion to consider compositional and microstructural changes induced by plastic deformation of the surfaces in frictional contact. Godet gave two definitions of the third body. The first definition was based on materials science and considered the third body as the zone with significant difference in chemical composition compared to the base material, see Fig. 1. First and second bodies are the base materials. The second definition was based on kinematic aspects where the third body is the near surface material layer that accommodates the differences in velocity between the first bodies. This definition was refined in 1989 [7,8] now distinguishing five sites of velocity accommodation, namely the two first bodies, the third body bulk and two interfaces called first body screens between third and first bodies.

Based on experimental data, Godet [7] suggested different phases of the running in starting with the mechanical interaction of two bodies and the initiation of first body structural changes. The formation of debris results in a three body contact and may lead to steady state conditions. The three body contact enables low friction and wear rate. In 2002 Berthier [9,10] introduced the

* Corresponding author at: Fraunhofer Institute for Mechanics of Materials IWM, MicroTribology Center μTC, Wöhlerstr. 11, 79108 Freiburg, Germany.
E-mail address: dominic.linsler@iwm.fraunhofer.de (D. Linsler).

model of the tribological circuit and defined different third body flows. One of them is the source flow originating from detached first and second body particles forming the third body. Another flow was called the internal flow describing the flow between first and second bodies and vice versa. A third major flow was called external source flow. For this kind of flow the constituents of oil or grease act as a source. Finally, the ejection flow corresponding to the loss of third body material was defined. The material ejected from the contact no longer participates in velocity accommodation. Wear was defined as the removal of first and second body material due to high source flow or because of high ejection flow. The reduction of the third body reactivates the source flow.

The understanding of the running in behavior, i.e., the change of friction and wear rate over time [11 14] is a necessary precondition for all life time predictions. It is therefore necessary to furnish the instructive models of Godet and Berthier with numbers on friction, wear rate, chemistry and structure of the third body. In addition, the localization of shear, i.e., the identification of the zone where velocity is accommodated, would provide insight into the kinetics of the running in.

Because of the highly dynamic tribological processes, continuous wear measurement with radionuclide technique (RNT) was used to determine the wear rate of the pin [15,16]. To observe running in and third body phenomena, samples were tested at constant load and speed and analyzed by microscopy and spectroscopy, see Fig. 1. For the visualization of velocity accommodation, different kinds of markers were prepared. Shear directly at the interface of the third body was monitored after implantation of Ga ions with the focused ion beam (FIB) followed by mappings with Auger electron spectroscopy (AES). To illustrate shear inside first and second body, platinum markers [17] were buried into the surface and analyzed after testing with FIB. The chemical composition of the third body was analyzed using photoelectron spectroscopy depth profiles (XPS).

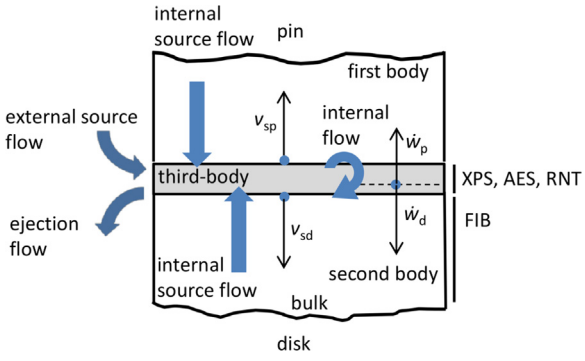

Fig. 1. The model according to Godet and Berthier. The growth rate of the tribological transitions v_s is always higher than the wear rate $\dot{w}$. The indices 'd' and 'p' denominate disk and pin, respectively.

Table 1
Elemental composition of the used Al-alloy.

Element	Si	Cu	Fe	Zn	Mg	Mn, Pb, Ti	Sr	Al
Conc. in weight (%)	10.6	2.5	0.9	0.8	0.2	< 0.2	200 ppm	Balance

2. Materials and methods

2.1. Materials

2.1.1. Disks

The composition of the strontium refined base alloy with a fine fibrous network of silicon [18,19] is shown in Table 1. A part of the disks was subjected to a heat treatment (solution heat treatment at 480 °C for 5 h followed by artificial aging at 180 °C for 4 h). These disks were called $AlSi_{HT}$. The not treated disks were called AlSi. The heat treatment resulted in a coarse globular Si phase, see Fig. 2.

Disks with a diameter of 50 mm and a thickness of 4.8 mm were machined from die cast cuboids. The machining comprised turning and milling steps. The finish was performed with a Wiper cutting insert. Topography was measured with white light interferometry showing that the finishing process generated defect free surfaces with reproducibly small roughnesses, see Fig. 3. In addition to topography, nanohardness was measured using a G 200 Nanoindenter XP (Agilent Technologies) operated in a continuous stiffness measurement mode. A Berkovich tip was indented at a constant strain rate of 0.025 s^{-1} to a depth of 2 μm. 75 indents per sample were performed.

Finally, X ray photoelectron spectroscopy (XPS) depth profiles were recorded to characterize the impact of machining and heat

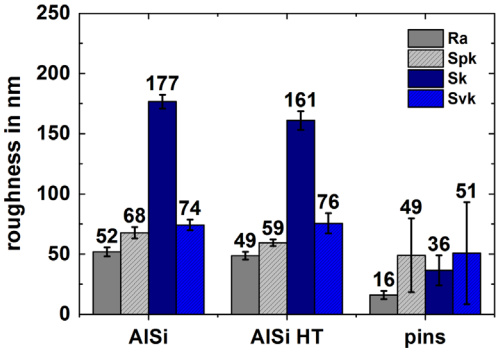

Fig. 3. Surface roughness values of unworn disks and pins. HT heat treatment. R_a: profile average roughness; S_{pk}: area reduced peak height; S_k: area core roughness; S_{vk}: area reduced valley depth.

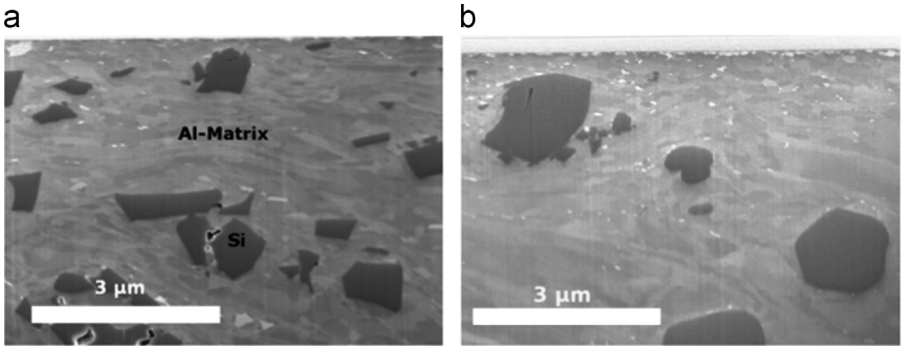

Fig. 2. SEM images of FIB cross sections in the unworn surfaces. The dark grains in the micrographs were identified as the Silicon phase, which is embedded in the Al matrix (gray). (a) AlSi disk without heat treatment. (b) AlSi disk with heat treatment.

treatment on the near surface concentration of silicon. Matrix concentration of silicon was achieved at a depth of about 300 nm. The heat treated disks showed matrix concentration at approxi mately 700 nm.

2.1.2. Pins

The pins were milled out of a 100Cr6 disk that was bandfinished in a two step process (Supfina™). The measured roughness values are shown in Fig. 3. FIB cross sections of the unworn pins showed a deformed subsurface microstructure up to a depth of 3.5 µm. The pins have a diameter of 5 mm. The edge of the pins was slightly tapered to prevent an undesired cutting into the disk. To achieve a flat contact between pin and disk the pin holder allowed a self regulating adjustment. For each test, new pins and disks were used.

2.1.3. Oil

The oil used for all pin on disk experiments was fully formu lated engine oil Castrol Edge FST 5W30 at a temperature of 70 °C. The oil circuit was filled with 4 l. Using a nozzle, oil was directly supplied to the disk.

2.2. Methods

2.2.1. Radionuclide technique

When measuring wear with the radionuclide technique (RNT), first and/or second body can be marked radioactively. The activity is extremely low, requiring the test setup to be shielded with lead. Due to wear, radioactive particles can be found in the oil. The activity in the oil is measured and correlated to the mass of the wear particles after calibration. The advantages of the method are its high resolution of a few micrograms per liter oil and the ability to measure wear continuously [4]. To obtain wear tracers, pins were subjected to low energy neutron radiation at FRM II in Munich. Upon tribological stressing nanometer sized wear parti cles are generated [20]. The oil circuit of the tribometer was connected to a gamma detector (Zyklotron AG) allowing contin uous monitoring of wear in the oil. Cr 51 was used as tracer element. To account for decay effects, a reference measuring device was included in the oil circulation. With the RNT, micro grams of wear can be detected in the oil circuit which corre sponds to a wear rate of a few nanometers per hour.

2.2.2. Focused ion beam

Besides the preparation of cross sections, FIB (FEI Helios 650 and Zeiss Crossbeam 1540) was used to introduce markers to investigate near surface as well as subsurface shear. To place the near surface gallium markers, a rectangular area (80 × 100 µm) inside a wear track was exposed to 30 keV Ga+ ion bombardment in deposition mode with a milling current of 200 pA for 6000 s. A topography scan of bombarded and adjacent area with atomic force microscopy showed a slight increase in roughness but no material removal.

To document shear behavior in deeper regions, markers [17] in form of trenches with a depth of six micrometers were introduced to disk and pin. The width of the trenches was two micrometers and their length was ten micrometers. The trenches were filled with the decomposition products of the platinum precursor gas (the expression platinum is used in the following for ease of reading).

2.2.3. XPS and AES

XPS depth profiles were recorded with a PHI 5000 Versaprobe system with 15 keV monochromatic Al Kα X ray excitation and an energy resolution of 0.2 eV. AES was measured with a PHI 680 Xi Auger Nanoprobe equipped with a field emission gun. Spectra were excited with 10 keV and 20 nA. Argon ions were used for material removal for depth profiling. The sputter rate was deter mined by means of a silicon oxide reference, yielding comparable values with an error in the depth values of about 10%. The area exposed to argon ions was about 2 × 2 mm^2. Photoelectrons were excited from an area of 200 × 300 µm^2 so that sample inhomo geneities do not have to be considered.

3. Results

3.1. Friction and wear

Friction experiments were conducted on a pin on disk trib ometer (Tetra GmbH) with a sliding velocity of 2 m/s and a contact pressure of 45 MPa.

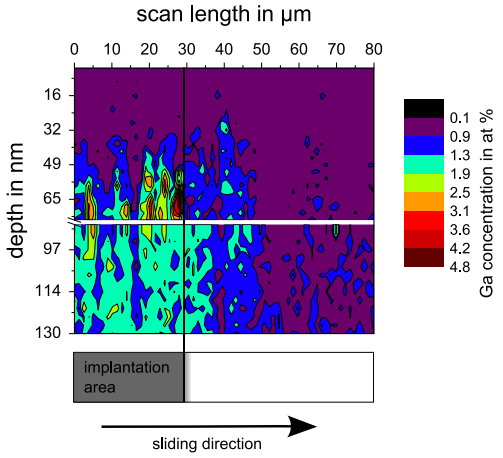

Fig. 5. Gallium concentrations from line profiles measured with AES as a function of sputter depth.

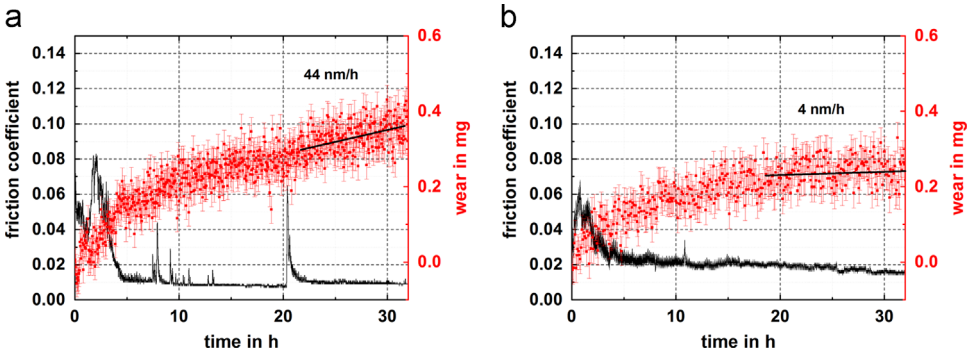

Fig. 4. Friction and wear curves. (a) AlSi disk without heat treatment. (b) AlSi disk with heat treatment.

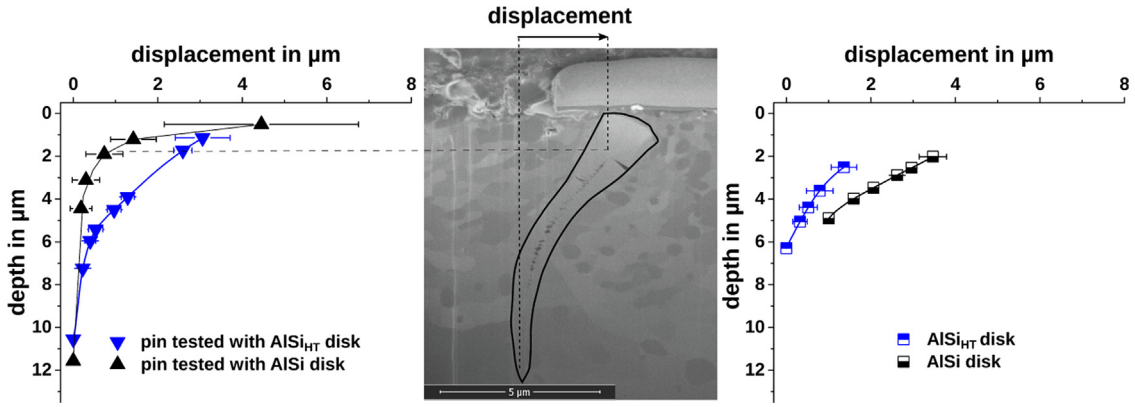

Fig. 6. Shear-induced displacements in pin (left) and disk (right). The inset shows the determination of the displacement.

The tested systems showed a distinct running in behavior with an initial coefficient of friction of 0.04 that decreased in the course of the experiment to 0.01. Wear of the pin was continuously measured with RNT. For both RNT experiments and its repetitions a constant slope of the wear signal in the last part of the running in allowed the calculation of the wear rate. The friction and wear signals are shown in Fig. 4. It is obvious that the systems developed clearly different wear rates, i.e. 4 nm/h for the heat treated system and 44 nm/h for the system without heat treatment. The scatter of the wear signal was caused by the random nature of radioactive decay. Wear of the disks was determined by white light interfero metry after the test. The linear wear rate the quotient of wear track depth and runtime was in the same range as the pins.

3.2. Analysis of the shear induced features

3.2.1. Structural analysis of near surface region

With the gallium implanted disk a 1200 m sliding test with the stressing conditions mentioned above was performed to analyze the initial stages of shear. After the run an AES linescan was placed alongside the wear track. The scan length (80 µm) was large enough to cover the border line between gallium implanted and base material. The linescan was expanded to a depth profile, by taking additional linescans after repeated removals of 3 nm of material. The total depth of the profile was 130 nm. Gallium was found beginning at a depth of 30 nm. In addition to the implanted area, gallium was found next to it as well. The detected concentrations were above noise level. Traces of gallium were found more than 25 µm away from the implanted area, see Fig. 5. This is significantly more than the lateral uncertainty of the Ga implantation field of 5 µm.

3.2.2. Structural analysis of subsurface region

In order to quantify shear in deeper ranges, the displacement of the center of the marker with respect to its initial position was taken as indicator, see Fig. 6. The platinum markers clearly indicated shear in the subsurface region, however, material deformation was less pronounced for the heat treated disk. The deformation of the marker placed in the pin was comparable with the displacement of the marker in the disk, in both cases approximately 4 µm.

The marker displacement in the pin exhibits its largest values in the range between surface and 1 µm. The pin run against the heat treated disk showed larger displacements for deeper regions. At the surface as well as for a depth larger than 10 µm the marker displacements in both pins were equal. The sliding distance of both marker experiments was 1200 m corresponding to approx. 30 min. The speed of the test with the heat treatment was adjusted so that the total work of friction was comparable for both experiments.

3.2.3. Chemical analysis of near surface and subsurface region

XPS depth profiles were recorded to analyze the near surface region and to show signs of mechanical intermixing without inter pretation of tribo chemical reactions. The measurements were con ducted on pins and disks. The depth profiles of worn disks and the associated pins showed the introduction of foreign elements from the oil (C and CH_x) and anti wear additives (S, P, Zn). The element Ca originated from detergents.

All tribologically stressed disks showed higher Si concentra tions in the near surface region than it was determined for the unworn state. Signs of oxidation are documented by the oxygen concentration. The depth profiles of the AlSi disk with and without heat treatment and of their pins are shown in Fig. 7. The spectra mainly differ in oxygen concentration. The near surface range of the disk without heat treatment contains significantly more oxygen. Accordingly, the aluminum concentration has a large oxydic fraction. For the pins the opposite case was determined. The pin run against the AlSi$_{HT}$ disk shows the higher oxygen content. In order to extract a typical depth value from the profiles, the point where oxygen reached 10% was taken. For the disks comparable values were received, whereas for the pin operated against AlSi$_{HT}$ a significantly greater depth was measured.

4. Discussion

4.1. Tribological flows

The discussion to explain the different wear rates is based on the excellent third body model developed by Godet and Berthier describ ing the mass flows in a tribological interface. In addition, to consider the energy flows in the interface, a balance is introduced [21]:

$$\dot{E}_{tot}(t) = \mu(t)F_n v = \dot{E}_q(t) + \dot{E}_w(t) + \dot{E}_m(t) \quad (1)$$

The total power of friction $\dot{E}_{tot}$ can be received by multiplication of coefficient of friction, normal force F_n and sliding velocity v. At the right side of the equation the resulting energy flows are shown. The total power of friction triggers a heat flow $\dot{E}_q$, the generation of wear $\dot{E}_w$ and the change of material involved in third body interactions $\dot{E}_m$. Except for normal force and sliding velocity all entities change with time. This is the impact of the running in. Since the friction behavior of both systems is very similar, see Fig. 4, the total power of friction is comparable. The systems differ in the microstructure of AlSi only. Thus, the portion of energy spent on heat generation should be comparable as well. What clearly differs is the energy portion that leads to wear. In [21] it was shown that the amount of energy that is transformed into heat ranges between 70% and 80%. Only a fraction often less than 1% contributes to wear. As a consequence, between 20% and 30% of the energy is

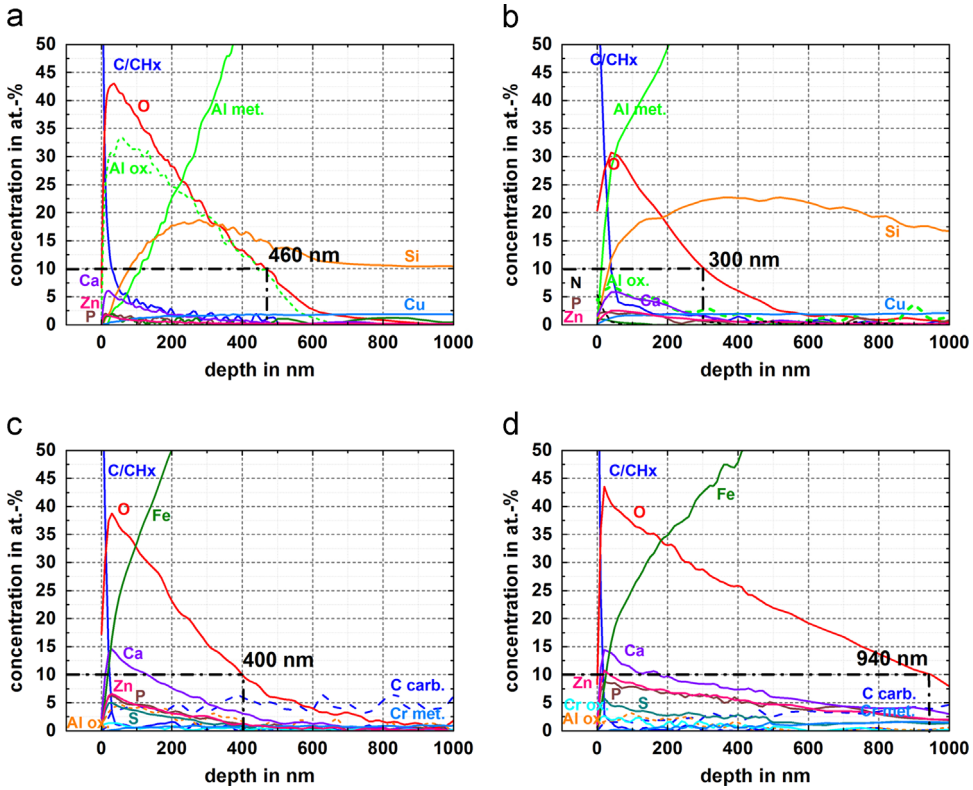

Fig. 7. XPS depth profiles. (a) AlSi disk without heat treatment. (b) AlSi disk with heat treatment. (c) Pin run against the AlSi disk without heat treatment. (d) Pin run against the AlSi disk with heat treatment.

consumed by third body interactions. With respect to the energy balance, differences in $\dot{E}_m$ should be visible in the properties of the third body, i.e., near surface microstructure and chemical composi tion. Changes in microstructure influence the deformation behavior of the materials which was clearly demonstrated by the platinum marker experiments. The AlSi disk that received the T6 heat treatment showed less deformation than the disk without heat treatment. The flowing characteristics of near and subsurface material was obviously changed. Due to larger Si crystals the mobility of the material was decreased. As a result, the deformation was transferred to the pin. The intensity of mechanical interaction was also documented by the penetration depth of oxygen into the near surface material of pin and disk. When the material is less mobile, as for $AlSi_{HT}$, oxygen cannot be found as deep as for the disk without heat treatment. However, the major difference in oxygen depth was measured for the pins, underlining the larger deforma tion of the pin run against the more resistant heat treated disk. The mechanical interaction of the $AlSi_{HT}$ system, this means its internal flow, was more intense than in the AlSi system which in turn leads to a reduced ejection flow, i.e., smaller wear rate and to a more pronounced third body as shown by XPS.

The wear curves underline that up to a runtime of 5 h the ejection flows were comparable. It is therefore concluded that the source flows, i.e., the flows of material from the first and second body into the third body, were comparable as well. After 5 h the largest amount of friction power was consumed. At the same time the wear curves began to deviate. The energy balance still holds, but with smaller magnitudes of $\dot{E}_q, \dot{E}_w$ and $\dot{E}_m$. The intensity of interaction decreased and the constant wear rates towards the end of the run suggest that source flows and ejection flow grew constant.

4.2. *Localization of shear*

Gallium ion markers were introduced to image the displacement of material at the near surface, i.e., directly at the third body interface between both solids. After tribological stressing no gallium ions were present up to a depth of 30 nm. In addition, traces of gallium were found up to 25 μm away from the area they were originally placed. This means that mechanical intermixing involves lateral mass transfer from one location of the friction body to another, the introduction of foreign elements, transfer and incorporation of mass originating from the counter body and the re incorporation of wear particles.

The gallium ion markers and their surrounding mass were displaced with a velocity of about 50 μm per hour (according to the experimental boundary conditions discussed above). Thus, wear particles do not originate from a resting and solid third body but from a highly mobile flowing pasty type of material. In the framework of Bowden Tabor theory (friction force = shear coefficient × real con tact area) this kind of newly formed material has a smaller shear coefficient than the base material. This means that the decrease in friction during running in is based on the formation of the third body, on its part connected with decreasing shear coefficient. After achiev ing constant wear rate, the third body gradually moves into first and second body with a velocity equal to the wear rate and the thickness of the third body is conserved until the systems fails due to fatigue. Only when first and second bodies are made of the same material, the velocity that shifts the third body is equal.

The mass leaving the interface forms the ejection flow. A wear rate of 4 nm/h insinuates that wear is composed of single atoms or groups of atoms. However, nanometer sized particles with a thick ness between 10 nm and 30 nm are generated and ejected [20]. Experiments by Dienwiebel et al. suggest that the wear mechanism is nano fatigue [22]. Due to intense internal flow in the third body, wear particles become re integrated, agglomerate and become ejected later. Interestingly, the time constants for achieving con stant friction and wear rate differ. The coefficient of friction reached its lowest values long before wear adopted constant wear rates.

The comparison of the sliding distance with the measured displacement of the Ga marker shows that more than 99.99% of the displacement are accommodated by the oil and the third body. We

therefore conclude that friction is determined by the shear properties of the near surface material, whereas wear involves subsurface regions of the material, as shown by the marker experiments characterizing the shear behavior at the beginning and the XPS depth profiles taken after full runtime at the end of the experiment.

5. Conclusions

The following conclusions can be drawn:

1. The initial subsurface morphology clearly influences the running in of the system. A second hard phase inside a ductile matrix impose a large impact on the flow behavior in mechanical intermixing.
2. Ultra low wear rates are possible, when the internal flow is intense and dominates. As soon as internal source flow or ejection flow dominate, wear increases.
3. The process of third body formation is time consuming.
4. A system that allows intense internal flows will show better performance with respect to wear, provided the material is not fatiguing.
5. For the present system friction is determined by the properties of the near surface region with a thickness up to 1 μm.
6. Godet's third body approach also applies for the processes taking place in the ultra low wear regime.

Acknowledgments

The authors would like to thank M. Haesche and M. Häuser (Fraunhofer IFAM) for casting and T. Schmidt (Fraunhofer IWU) for the machining of the disks. Thanks are also due to E. Nold (Fraunhofer IWM) for XPS measurements, P. Brenner (KIT LEM) for a part of the FIB work and R. Schwaiger and I. Bernstein (KIT) for their support in nanoindentation measurements. We acknowl edge the support of the German Science Foundation (SPP 1551).

References

[1] J. Walker, W. Rainforth, H. Jones, Lubricated sliding wear behaviour of aluminium alloy composites, Wear 259 (1–6) (2005) 577–589.
[2] S. Dey, M. Lukitsch, M. Balogh, X. Meng-Burany, A. Alpas, Ultra-mild wear mechanisms of al12.6 si alloys at elevated temperature, Wear 271 (9–10) (2011) 1842–1853.
[3] M. Dienwiebel, K. Pöhlmann, M. Scherge, Origins of the wear resistance of alsi cylinder bore surfaces studies by surface analytical tools, Tribol. Int. 260 (2007) 458–461.
[4] M. Scherge, D. Shakhvorostov, K. Pöhlmann, Fundamental wear mechanisms of metals, Wear 255 (2003) 395–400.
[5] D. Rigney, J. Hirth, Plastic deformation and sliding friction of metals, Wear 53 (1979) 345–370.
[6] M. Godet, The third-body approach: a mechanical view of wear, Wear 100 (1984) 437–452.
[7] M. Godet, Third-bodies in tribology, Wear 136 (1990) 29–45.
[8] Y. Berthier, M. Godet, M. Brendle, Velocity accommodation in friction, Tribol. Trans. 32 (1989) 490–496.
[9] Y. Berthier, Wear—Materials, Mechanisms and Practice, Wiley, Chichester, 2005, pp. 291–316 (Chapter 12: Third Body Reality—Consequences and Use of the Third-Body Concept to Solve Friction and Wear Problems).
[10] S. Descartes, Y. Berthier, Rheology and flows of solid third bodies: background and application to an MoS1.6 coating, Wear 252 (2002) 546–556.
[11] B. Jacobson, The stribeck memorial lecture, Tribol. Int. 36 (2003) 781–789. http://dx.doi.org/10.1016/S0301-679X(03)00094-X.
[12] J. Volz, Erstellung optimierter Einlaufprogramme von Dieselmotoren, Universitaet Karlsruhe, Kernforschungszentrum Karlsruhe KFK 2432, 1977.
[13] E. Corniani, M. Jech, T. Wopelka, F. Ditroi, F. Franek, A. Pauschitz, High-resolution wear analysis of a ball-on-disc contact using low-activity radioactive isotopes, Proc. IMechE Part C: J. Mech. Eng. 226 (2) (2011) 319–326. http://dx.doi.org/10.1177/0954406211424865.
[14] D. Shakhvorostov, A. Lachenwitzer, L. Coatsworth, W. Lennard, P. Norton, Correlated wear measurements using gold implantation, backscattering, nuclear activation analysis and profilometry, Tribol. Int. 44 (2011) 737–750. http://dx.doi.org/10.1016/j.triboint.2009.12.011.
[15] A. Gervé, Modern use of radioisotopes in wear measurement, J. Mater. Technol. 3 (2) (1972) 81–86 (in German).
[16] M. Scherge, K. Pöhlmann, A. Gervé, Wear measurement using radionuclide-technique (RNT), Wear 254 (2003) 801–817.
[17] D. Persson, On the mechanisms behind the tribological performance of stellites, Uppsala University, Acta Universitatis Upsaliensis, 2005, ISBN 91–554–6420–3.
[18] F. Lasagni, A. Lasagni, E. Marks, C. Holzapfel, F. Mücklich, H. Degischer, Three-dimensional characterization of ascast and solution-treated AlSi12(Ssr) alloys by high-resolution FIB tomography, Acta Mater. 55 (2007) 3875–3882. http://dx.doi.org/10.1016/j.actamat.2007.03.004.
[19] M. Timpel, N. Wanderkaa, R. Schlesiger, T. Yamamotoc, D. Isheim, G. Schmitz, S. Matsumurac, J. Banhart, Sr–Al–Si co-segregated regions in eutectic Si phase of Sr-modified Al–10Si alloy, Ultramicroscopy 132 (2013) 216–221. http://dx.doi.org/10.1016/j.ultramic.2012.10.006.
[20] M. Scherge, J. Martin, K. Pöhlmann, Characterization of wear debris of systems operated under low wear-rate conditions, Wear 260 (2006) 458–461.
[21] D. Shakhvorostov, K. Pöhlmann, M. Scherge, An energetic approach to friction, wear and temperature, Wear 257 (2004) 124–130.
[22] S. Korres, T. Feser, M. Dienwiebel, In situ observation of wear particle formation on lubricated sliding surfaces, Acta Mater. 60 (2012) 420–429.